# Aeronomic effects of the solar flares in the topside ionosphere

L. A. Leonovich and A. V. Taschilin

*Institute of Solar-Terrestrial Physics, Russian Academy of Sciences SB RAS, 664033 p/o box 4026, Irkutsk, Russia*

(Received October 23, 2007; Revised February 22, 2008; Accepted March 20, 2008; Online published May 29, 2009)

We obtained that according to the GPS data at altitudes of the topside ionosphere ($h > 300$ km) a flare is able to cause a decrease of the electron content. Using the theoretical model it is shown that the intense transport of $O^+$ ions into the above-situated plasma caused by a sharp increase in the ion production rate and thermal expansion of the ionospheric plasma is a cause of the formation of the negative disturbance in the electron concentration in the topside ionosphere.

**Key words:** Solar flares, disturbances, ionosphere, GPS, modeling.

## 1. Observations of the TEC Variations during a Powerful Flare on 14 July 2000

Phase measurements of GPS signals make it possible to obtain variations of TEC along the receiver-satellite path, Fitzgerald (1997), Hoffmann-Wellenhof *et al*. (1992), Klobuchar (1986). Knowing variations in TEC, one is able to evaluate the changes in the total electron content above some given level, using the method based on the effects of partial "shadowing" of the atmosphere by the globe, Leonovich *et al*. (2002).

Now we consider the results of application of the method fore-quoted to studies of the ionospheric effects of the powerful solar flare X5.7/3B registered on 14 July 2000 at 1024 UT (N22W07) on the background of quiet geomagnetic situation ($D_{st} = -10$ nT). Figure 1(a) shows the time behavior of the energy flux of the soft X rays in the 0.1–0.8 nm range (the data from the GOES 10 satellite) for the flare in consideration. Vertical dashed lines show the beginning of the flare and the time when the X-ray flux was maximal. The corresponding variations in TEC along rays directed to the GPS satellites and crossing the shadow boundary at various heights $h_0$ during the flare are shown in Figs. 1(b)–1(f).

One can see in Fig. 1(b) that the total electron content within the entire ionosphere ($h_0 = 0$) for the IRKT station located in the sunlit hemisphere starts to grow from the moment of the flare beginning (1012 UT) and lasts till 1036 UT. At the ray crossing the shadow region at a height of 240 km (Fig. 1(c)), the TEC grow begins some time after the flare beginning in the soft X-ray range. Similar picture is seen at other rays satisfying the condition $h_0 < 380$ km. At the same time, for the rays with $h_0 \geq 380$ km (Figs. 1(d)–1(e)) a decrease in the electron content above the $h_0$ level occurs after the flare beginning (1012 UT) and lasts till 1024 UT, i.e., till the moment of the flare maximum in the soft X-ray range.



Similar decrease in the electron content after the beginning of a solar flare was detected in ionospheric observations using the incoherent scatter radar at Arecibo, Thome and Wagner (1981). During two solar flares on 21 and 23 May 1967, negative disturbances of the electron concentration with an amplitude from 3% to 10% were registered within the height interval 280–600 km. The goal of this paper is studying mechanism of electron concentration negative disturbances in the topside ionosphere caused by solar flares.

## 2. Results of the Model Calculations of the Ionosphere Behavior during a Solar Flare

For studying physical processes governing ionospheric effects of solar flares, we used the model of the ionosphere-plasmasphere interaction, Krinberg and Taschilin (1984). The model makes it possible to calculate time variations of the ion composition, temperature, and also of the fluxes of particles and heat in the conjugated ionospheres. The model is based on numerical solution of the nonstationary equations of the balance of particles and energy of the thermal plasma within closed magnetic field tubes, their bases lying at a height $h = 100$ km. It is assumed that the ionospheric plasma consists of electrons and atomic ions $H^+$ and $O^+$, and also of molecular ions $NO^+$, $N_2^+$, and $O_2^+$. The UV-radiation spectrum by Richards *et al*. (1994) and the X-ray radiation spectrum by Nusinov (1992) were used for the calculation of the photoionization rates of the thermospheric constituents O, $O_2$, and $N_2$ and energetic spectra of the primary photoelectrons in undisturbed conditions (without a flare). The MSIS 86, Hedin *et al*. (1991), global empirical model of the thermosphere was used for the description of the spatial-time variations of the atmospheric temperature and concentrations of the neutral components O, $O_2$, $N_2$, and H.

For studying the flare effects, a disturbed model of the solar radiation spectrum in the X-ray and UV ranges was created. According to the existence of the pulse and slow phases of a flare, we assumed that the spectrum within the wavelength interval 0.1–10 nm stays disturbed during 36

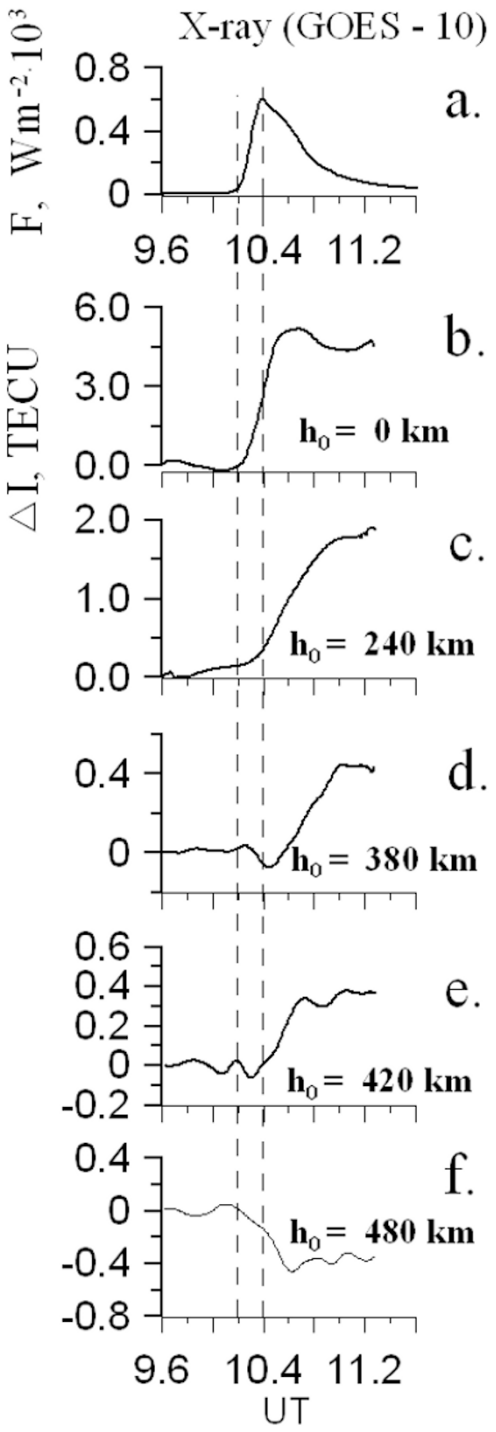


Fig. 1. Results of the TEC response according to the GPS measurements. Time profiles of the soft X-ray radiation within the 1–8 Å range (the data of the GOES 10 satellite) during the solar flare on 14 July 2000 (a). Examples of the TEC responses to the solar flare measured at the rays (between ground-based stations and GPS satellite) crossing the boundary of the Earth's shadow cone at different altitudes $h_0$ (b–f).

minutes (the slow phase), whereas the pulse phase (for the 10–105 nm interval) lasts during 15 minutes. We also assumed that the spectrum is disturbed instantly and stays constant during the above indicated time intervals, switching off instantly after that. To give the value of the disturbance of the solar energy flux, the entire wavelength interval was split to 6 parts. For each part the most typical value of the intensity factor, Avakyan *et al*. (1994), Horan and Kreplin (1981), Korenkov and Namgaladze (1977), was found. The value was determined as the ratio of the energy flux during the flare to the radiation flux of the quiet Sun. Table 1 shows values of the flare intensity factors for each spectral interval.

Table 1. Increase in the solar radiation intensity for particular spectral intervals during the flare.

| Intervals, nm | 0.1–0.8 | 0.8–2 | 2–4 | 4–6 | 6–10 | 10–105 |
|---|---|---|---|---|---|---|
| Intensity factor | 1000 | 100 | 50 | 20 | 4 | 1.3 |

The reaction of the midlatitude ionosphere to a considered solar flare was simulated by calculating the variations of plasma parameters within the geomagnetic field tube. The calculation was performed for the period 10–15 July 2000, using arbitrary initial conditions corresponding to low content of the thermal plasma in the tube. The considered time period was characterized by high level of solar activity ($F_{10.7} \approx 210$). The model calculation results of height-time variations of the electron concentration for different conditions of solar irradiating intensity are shown in Figs. 2, (2(a)–2(f))—for the terminator area and (2(g)–2(l))—for the local noon. The moment of a solar flare beginning is shown by vertical dashed lines.

The character of the time behavior of $N_e$ changes principally above the $F_2$ layer. One can see in Figs. 2(d)–2(f) and 2(j)–2(l) that within the height interval 380–600 km instead of the electron concentration increase after the flare beginning, a trough is formed in the time behavior of $N_e$. The value of the $N_e$ decrease amplitude lies within 1–5%. It should be noted that the obtained in the calculations negative disturbance of the electron concentration in the topside ionosphere agrees well to the presented above TEC variations obtained as a result of processing of GPS signals and in observations at the Arecibo incoherent scatter radar Thome and Wagner (1981). Thus, one can conclude that the conditions during a solar flare could be such that an increase of the electron concentration occurs in the lower ionosphere, but in the topside ionosphere $N_e$ decreases.

## 3. Discussion of the Modeling Results

In order to find the causes of formation of the electron concentration negative disturbance in the topside ionosphere, we assumed that the $N_e$ decrease is related to inhomogeneous variations of the ultraviolet radiation in various parts of the spectrum during a flare. On the basis of this assumption, the UV-radiation spectrum within the 10–105 nm range was split to 19 equal intervals. Then, for each interval in turn, the factor of flare radiation intensity was varied from 1.3 to 10, whereas for the other intervals it stayed equal to 1.3. The calculations showed that the effect of $N_e$ decrease after the beginning of a flare is pronounced best at the increase of the intensity factor in three following spectral intervals: 15–20 nm, 30–35 nm, and 35–40 nm.

In order to understand the physical causes of the electron concentration depletion at altitudes of the topside ionosphere, we consider the continuity equation for the iono-

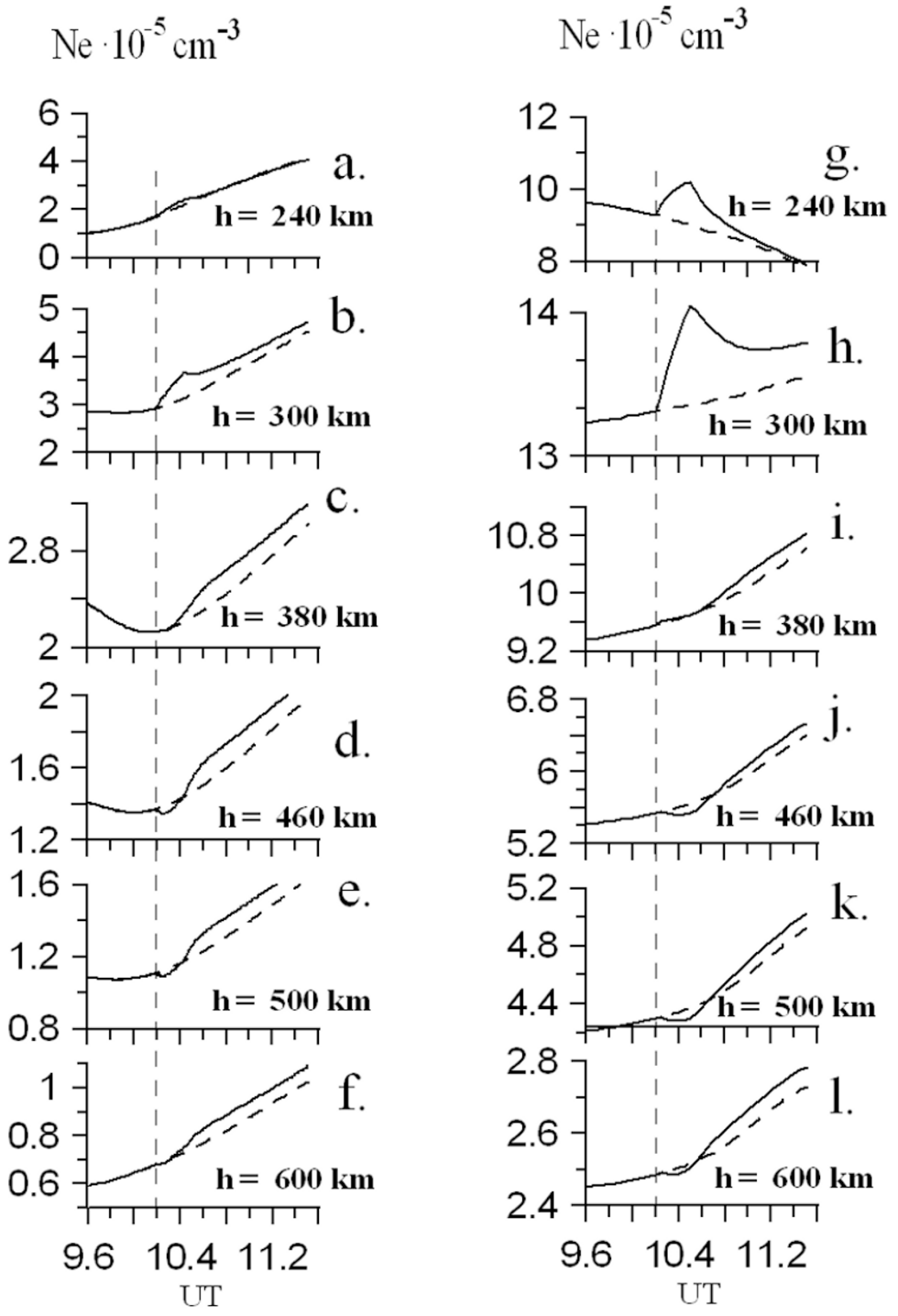


Fig. 2. The model calculation results of the height-time variations of the electron concentration for different conditions of solar irradiating intensity, (2(a)–2(f))—for the terminator area and (2(g)–2(l))—for the local noon. The dashed lines show variations of the electron concentration when solar flare misses. The moment of a solar flare beginning is shown by vertical dashed lines.

spheric plasma written in the form:

$$\frac{\partial N_e}{\partial t} = q - l_n - \mathrm{div}(\boldsymbol{W}), \qquad (1)$$

where $q$ is the ion production rate; $l_n$ is the loss rate of electron-ion pairs in chemical reactions; and $\boldsymbol{W}$ is the total ion flux along a geomagnetic field line. It follows from (1) that the sign of the $N_e$ changes is determined by the total balance of the terms in the right-hand side and that a negative disturbance to be formed the right-hand side of (1) should be negative during the flare. The results of the modeling make it possible to determine the processes providing realization of such situation.

Figure 3 shows the time variations of the electron concentration and particular terms of the right-hand side of Eq. (1) at a height of the $F_2$ layer (300 km) and in the topside iono-

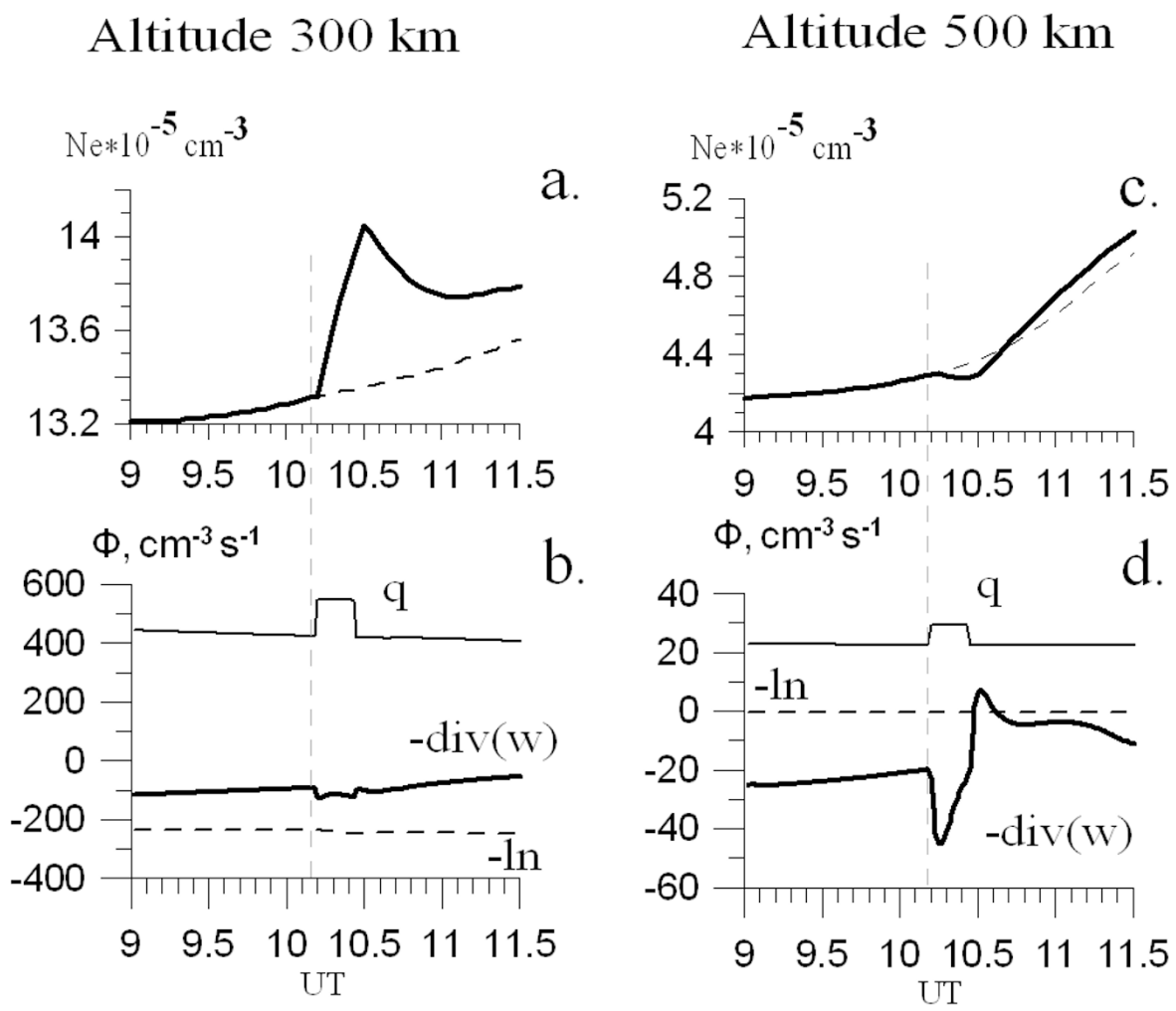


Fig. 3. Analysis of the effect of the decrease in the electron concentration during the solar flare. Thick lines show the time variations of the electron concentration during a solar flare at heights of 300 km (a) and 500 km (c), diamonds show the time variations of the electron concentration in the absence of the flare. The time variations of the terms in the continuity equation calculated for height 300 km (b) where the effect of the electron concentration depletion during the flare is not observed and 500 km (d) where the effect is clearly pronounced are also shown in the bottom panels.

sphere (500 km). It should be noted that within this height interval ions of the atomic oxygen prevail and so Eq. (1) actually describe the balance of $O^+$ ions. It follows from Fig. 3(b) that at a level of 300 km the value of ion production rate exceeds considerably the loss of charged particles due to the recombination $l_n$ and transport of $O^+$ ions along the field lines (div$\boldsymbol{W} > 0$). As a result, there occurs a monotonous increase in $N_e$ during a flare. After the end of the flare, the photoionization rate decreases sharply. Due to that, the electron concentration at first decreases sharply and then is stabilized at some level, the latter being determined by the balance between the photoionization, input of the $O^+$ ions from the above-located plasmasphere, and chemical loss.

At altitudes of the topside ionosphere (500 km), the relation between particular terms of the right-hand side of (1) changes. First, a decrease with height in the absolute values of the ion production rates and recombination occurs, and, second, the role of the diffuse transport of ions in the ionization balance grows. Figure 3(d) shows that the values of the divergence of ion flux rapidly increases on an absolute value with the beginning of the flare and becomes a predominating term in the right-hand side of Eq. (1). This happens due to the reformation of the vertical profile of the ion flux above the $F_2$-layer maximum with the beginning of the flare. After the sharp increase in the initial moment of the flare, the absolute value of the flux divergence decreases reaching the pre-flare value at the end of the pulse phase (Fig. 3(d)). Then a reversal of the flux divergence sign to the opposite one occurs accompanied by an increase of the electron concentration.

Figure 4 shows the vertical profiles of the ion flux before the flare and in the maximal phase of the flare. One can see that under undisturbed conditions ions $O^+$ are transported from the topside ionosphere through the $F_2$ layer into the lower ionosphere. During the maximal phase of the flare, the plasma pressure in the $F_2$ layer increases sharply and above $\sim$380 km an intense upward flux of $O^+$ ions into the plasmasphere is formed. As a result, at altitudes above $\sim$380 km the divergence of the ion flux is positive and considerable on quantity, that specifies on essential upward of plasma from the ionosphere to the plasmasphere.

Thus, one can conclude that the decrease of the electron concentration in the topside ionosphere is due to the bring-

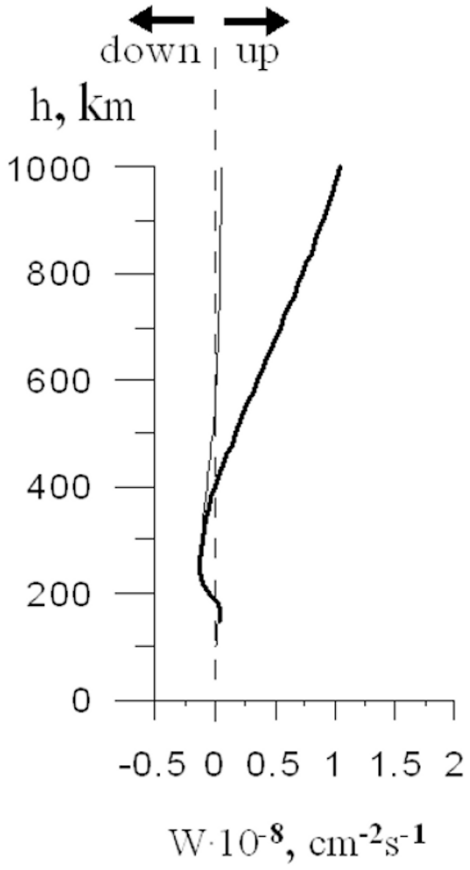


Fig. 4. Vertical profile of the flux $\boldsymbol{W}$. Thin line shows the flux behavior before the flare. Thick line shows the flux behavior during the flare.

ing out to the plasmasphere of $O^+$ ions. After "switching off" the flare, the plasma pressure in the $F_2$ layer decreases quickly down to the level at which the difference in the pressure between the upper and lower parts of the ionosphere can not any more support the upward flux of $O^+$ ions, and the ionosphere relaxes to the undisturbed state.

Now we consider the problem of length of the height interval in which the conditions needed to formation of the negative disturbance in $N_e$ are fulfilled. Figure 5 shows the vertical profiles of the particular terms in the right-hand side of Eq. (1) before a flare (Fig. 5(a)) and during the flare (Fig. 5(b)). In the same figures, the summated profile of all terms in the right-hand side of Eq. (1) is shown by triangles. One can see that in the absence of a solar flare in the daytime the resulting curve is positive at $h < 400$ km and is close to zero above 400 km, that is, in the topside ionosphere the condition $\partial N_e/\partial t \geq 0$ is fulfilled everywhere. During a flare the right-hand side of Eq. (1) takes negative values in the 380–600 km altitude range (is shown by horizontal dashed lines in Fig. 5). So it follows that a negative disturbance of the electron concentration during a flare can cover almost the entire topside ionosphere.

## 4. Conclusions

The response of the ionosphere to a solar flare is studied on the basis of the observational data and results of theoretical modeling. The analysis of the results obtained made it possible to draw the following conclusions:

1. According to the observations of the variations in TEC and electron concentration at the GPS receivers network and at the IS installation at Arecibo, negative disturbances of the electron concentration can be formed in the topside ionosphere during solar flares.
2. It is found in the model simulations that the most significant effect of the $N_e$ depletion is seen during the flares with a strong increase in the solar radiation within the following spectral intervals: 15–20 nm and 30–40 nm.
3. The intense transporting of $O^+$ ions up into the above-located plasmasphere is a cause of the formation of the

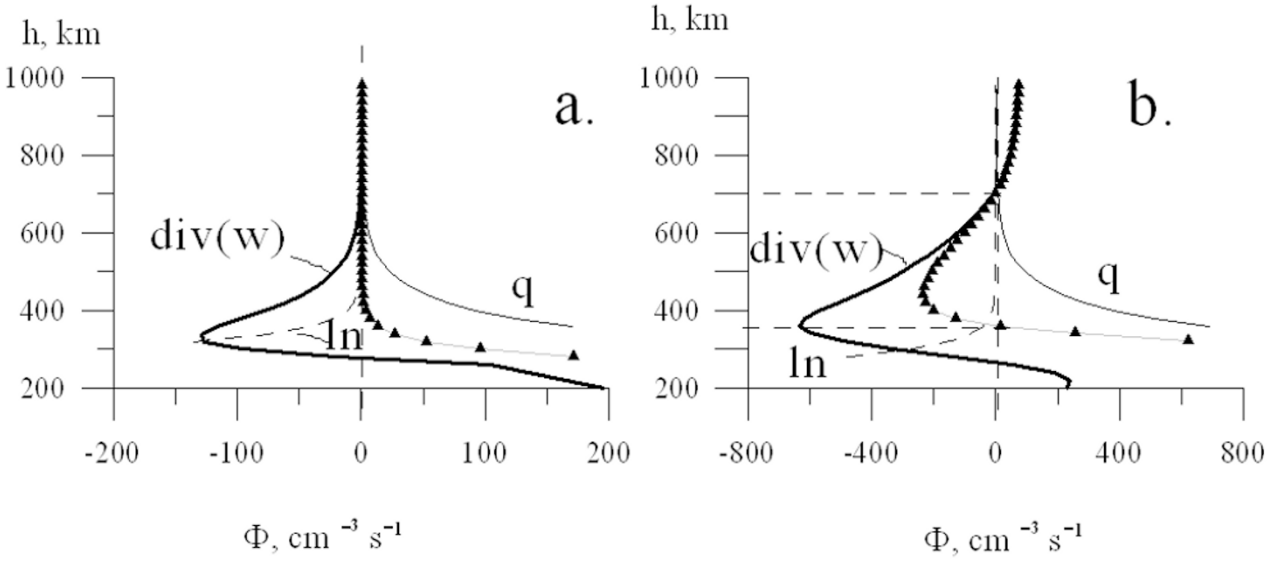


Fig. 5. Analysis of the continuity equation. Vertical profiles of the terms of the continuity equation before the flare (a) and during the flare (b). Thin curves show the electron formation rate $q$; dashed curves show the electron loss rate $l_n$; thick lines show the flux divergence div($\boldsymbol{W}$). The data for the loss rate and flux divergence are shown with negative signs as they enter to the considered equation. The curve with triangles is a resulting curve.

negative disturbance in $N_e$ in the topside ionosphere. The transporting is caused by the sharp increase in the ion production rate and in the thermal expansion of the ionospheric plasma.

**Acknowledgments.** The GPS data on the 14 July 2000 flare were kindly provided by E. L. Afraimovich and S. V. Voeikov. E. B. Romanova helped considerably in model simulations. We sincerely thank them all.

## References

Avakyan, S. V., A. I. Vdovin, and V. F. Pustarnakov, *Ionizing and Penetrating Radiation in the Near-Earth Space Environment*, 500 pp., Hydrometeoizdat, St.-Petersburg, 1994.

Fitzgerald, T. J., Observations of total electron content perturbations on GPS signals caused by a ground level explosion, *J. Atmos. Sol.-Terr. Phys.*, **59**, 829, 1997.

Hedin, A. E. *et al.*, Revised global model of thermosphere winds using satellite and ground-based observations, *J. Geophys. Res.*, **96**(5), 7657, 1991.

Hoffmann-Wellenhof, B., H. Lichtenegger, and J. Collins, *Global Positioning System: Theory and Practice*, Springer-Verlag, Wien, 1992.

Horan, D. M. and R. W. Kreplin, Simultaneous measurements of EUV and soft X-ray solar flare emission, *Sol. Phys.*, **74**(1), 265, doi:10.1007/BF00151295, 1981.

Klobuchar, J. A., Ionospheric time-delay algorithm for single-frequency GPS users, *IEEE Trans. Aero. Electron. Sys.*, **23**(3), 325, 1986.

Korenkov, Yu. N. and A. A. Namgaladze, Modelling of the ionospheric effects of the solar flares, in *Ionospheric disturbances and forecast methods*, edited by L. N. Lyhova and L. A. Yudovich, 228 pp., Moscow, Publ. House "Nauka", 1977.

Krinberg, I. A. and A. V. Taschilin, *Ionosphere and Plasmasphere*, Nauka, Moscow, 1984.

Leonovich, L. A., E. L. Afraimovich, E. B. Romanova, and A. V. Taschilin, Estimating the contribution from different ionospheric regions to the TEC response to the solar flares using data from the international GPS network, *Ann. Geophys.*, **20**, 1935, 2002.

Nusinov, A. A., Models for prediction of EUV and X ray solar radiation based on 10.7-cm radio emission, in *Proc. Workshop on Solar Electromagnetic Radiation for Solar Cycle 22*, Boulder, Colo., July 1992, edited by R. F. Donnely, NOAA ERL, Boulder, Colo., USA, 354, 1992.

Richards, P. G., J. A. Fennelly, and D. G. Tor, EUVAC: A solar EUV flux model for aeronomic calculations, *J. Geophys. Res.*, **99**, 8981, doi:10.1029/94JA00518, 1994.

Thome, G. D. and L. S. Wagner, Electron density enhancements in the E and F regions of the ionosphere during solar flares, *J. Geophys. Res.*, **76**, 6883, 1981.

L. A. Leonovich (e-mail: lal@iszf.irk.ru) and A. V. Taschilin